Chapter 12

Respiratory Metabolism in Heterotrophic Plant Cells as Revealed by Isotopic Labeling and Metabolic Flux Analysis

Martine Dieuaide-Noubhani* and Dominique Rolin
Biologie du Fruit et Pathologie, INRA, Université de Bordeaux, 33882 Villenave d'Ornon, UMR 1332, France

Summary

Mitochondrial respiration requires redox power that is mainly provided by the tricarboxylic acid (TCA) cycle in heterotrophic tissues. Glycolysis is commonly assumed to be the major pathway for carbon replenishment of the TCA cycle in most plant cells. However, the TCA cycle also provides precursors for amino acids and organic acids synthesis, a process that requires 4- or 5-C molecules supplied by anaplerotic pathways. The TCA cycle is thus involved in both anabolism and catabolism. Despite the good knowledge of enzymes and pathways involved in these processes, the regulation of carbon partitioning between catabolism and anabolism remains poorly understood. Metabolic flux analysis (MFA) aims at quantifying fluxes in metabolic networks and provides new insights for the study of the

*Author for Correspondence, e-mail: martine.dieuaide-noubhani@inra.fr

e-mail: dominique.rolin@inra.fr

G. Tcherkez, J. Ghashghaie (eds.), *Plant Respiration: Metabolic Fluxes and Carbon Balance*, Advances in Photosynthesis and Respiration 43, https://doi.org/10.1007/978-3-319-68703-2_12,

TCA cycle and associated pathways. This chapter presents briefly the principles of MFA, and describes how ^{14}C-tracing evolved to ^{13}C-MFA, and more recently to ^{13}C-INST-MFA. Such analyses have provided insights about the origin of carbon atoms entering the TCA cycle and the partitioning between respiration and biosyntheses.

I. Introduction

Heterotrophic plant cells import carbon mostly in the form of sucrose, and also as amino acids thereby sustaining nitrogen metabolism. Sucrose is a source of carbon for the biosynthesis of structural and storage compounds (proteins, lipids, free sugars, starch, organic acids) through anabolic pathways but also for respiration *via* glycolysis and the TCA cycle, hence generating ATP which is in turn utilized for biosynthesis or maintenance.

Therefore, the TCA cycle plays a pivotal role, being involved both in energy generation and biosynthetic processes. Phospho*enol*pyruvate (PEP) is a key intermediate produced in the cytosol by glycolysis and converted to pyruvate which enters the mitochondria to be further decarboxylated to acetyl-CoA by the pyruvate dehydrogenase complex (PDH). Acetyl-CoA then condenses with oxaloacetate (OAA) to produce citrate (see metabolic network Fig. 12.1). By the action of the TCA cycle, the 2 carbons unit (acetyl group) is fully oxidized to CO_2, with regeneration of OAA and the net production of NADH and $FADH_2$ that are used for respiration. The TCA cycle provides intermediates for the biosynthesis of amino acids and organic acids, such as 2-oxoglutarate (glutamate precursor) and oxaloacetate (aspartate precursor). Hence, to avoid the depletion of pools of TCA cycle intermediates, some carbon must be supplemented by pathways that are called 'anaplerotic' pathways.

In heterotrophic plant cells, the major source of anaplerotic carbon is PEP. The PEP carboxylase (PEPC), localized in the cytosol, catalyzes the production of OAA from PEP and bicarbonate (HCO_3^-). OAA is imported into the mitochondria and either *(i)* feeds the production of C_4 molecules such as amino acids of the aspartate family and malate, or *(ii)* combines with acetyl-CoA to produce citrate that can be accumulated in the vacuole or further transformed into the TCA cycle. Also, malate formed in the TCA cycle can be converted to pyruvate *via* the mitochondrial malic enzyme, thus providing substrate to the PDH. The complexity of that network and the multiple branching points raises several questions such as the origin of carbon atoms that are committed to the TCA cycle and the partitioning between anaplerotic pathways and respiration.

In the past last decades, the growing interest in metabolic engineering favored the development of methods to estimate fluxes in living cells. Several reviews (Baghalian et al. 2014; Dersch et al. 2016) described approaches involved and more recently, a book was dedicated to protocols associated with flux analysis in plants (Dieuaide-Nouhhani and Alonso 2014). In summary, three main methods are recognized: metabolic flux analysis (MFA), flux balance analysis (FBA) and kinetic models. ^{13}C- or ^{14}C-MFA is based on the use of ^{13}C- or ^{14}C-labeled precursors (also called tracers) that enter metabolism. The labeled carbon atoms are redistributed in metabolic pathways and the isotopic labeling in intracellular metabolites is measured by nuclear magnetic resonance (NMR) or mass spectrometry (MS). The analysis of labeling in metabolites (isotopic enrichment) with modeling allows the quantitation of fluxes associated with the metabolic reactions considered. The output is a flux map that

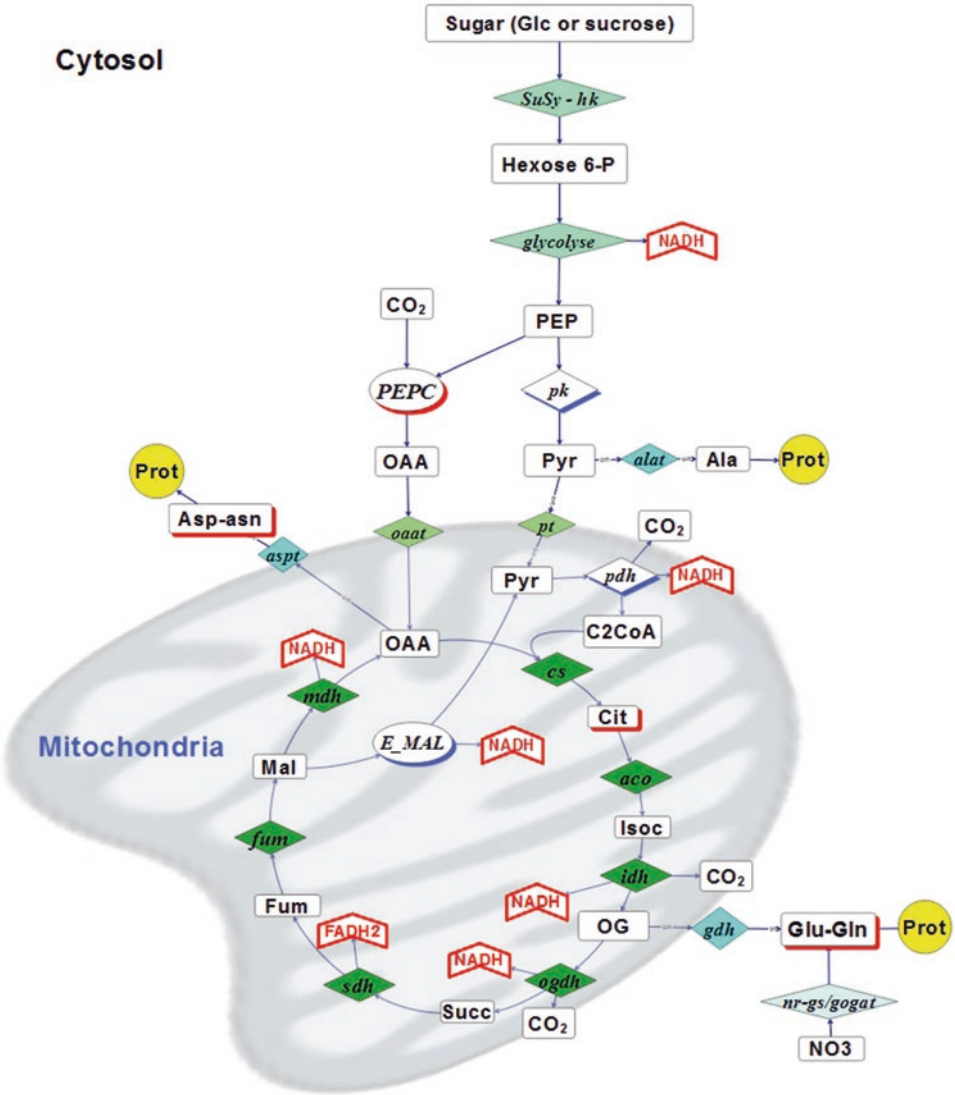

Fig. 12.1. **Simplified metabolic network.** Flux names are given in italics. Abbreviations: SuSy sucrose synthase, hk hexokinase, pk pyruvate kinase, oaat and pt are OAA and pyruvate transporters respectively, alat alanine aminotransferase, aspt aspartate aminotransferase, pdh pyruvate dehydrogenase, cs citrate synthase, aco aconitase, idh isocitrate dehydrogenase, ogdh 2-oxoglutarate dehydrogenase, sdh succinate dehydrogenase, fum fumarase, mdh malate dehydrogenase, nr: nitrate reductase, gdh glutamate dehydrogenase, gs/gogat glutamine synthase/glutamate synthase, PEPC phosphoenolpyruvate carboxylase, Glc glucose, PEP phosphoenolpyruvate, Pyr pyruvate, OAA oxaloacetate, Cit citrate, Icit isocitrate, OG 2-oxoglutarate, Succ succinate, Fum fumarate, Mal malate, Prot proteins. Standard abbreviations of amino acid names are used (The illustration was designed with OMIX (Droste et al. 2011))

shows the distribution of anabolic and catabolic fluxes over the metabolic network. FBA (Schuster et al. 1999) belongs to constraint-based modeling where relying on biochemical and genomic information, the metabolic network is constrained by reaction stoichiometry. Based on an assumed objective function, and by applying mass-balance constraints, fluxes can be predicted after linear optimization. In the last decade, recent

advances in reconstruction and applications of genome-scale metabolic models have been developed for the plant model *Arabidopsis thaliana* (de Oliveira Dal'Molin et al. 2010, 2015; Kim et al. 2012; Grafahrend-Belau et al. 2013) but also maize (Saha et al. 2011) and barley seeds (Grafahrend-Belau et al. 2009). Interestingly, using a restricted network focused on primary metabolism including energy and redox balance, FBA allowed estimating carbon and nitrogen needs for tomato fruit growth and anticipating the metabolic reprogramming along its development, from division phase to maturity (Colombié et al. 2015). The third approach, kinetic modeling, consists in a detailed and complicated mathematical description of a metabolic network. Kinetic modeling is based on known kinetic parameters and contents in enzymes. It represents now an important branch in the growing field of quantification of fluxes in metabolic networks. This approach has been used to study sucrose metabolism in sugarcane (Rohwer and Botha 2001), the compartmentalization of sugar metabolism in tomato (Beauvoit et al. 2014), and metabolic branching points between methionine and threonine biosynthesis (Curien et al. 2003) and in aspartate metabolism in *Arabidopsis thaliana* (Curien et al. 2009).

In this chapter, we will provide an overview of methods for flux quantification, from ^{14}C- to ^{13}C-MFA, and then review their application to respiratory metabolism in heterotrophic plant cells.

II. Labeling Experiments to Quantify Metabolic Flux in Heterotrophic Tissues of Plants: From Steady-State to Instationary MFA

A. Overview of ^{13}C- or ^{14}C-Labeling Techniques

Historically, metabolic flux analysis was first carried out using ^{14}C-labeled tracers. In lettuce seeds (*Lactuca sativa*), TCA cycle activity was assessed by modeling [U-^{14}C]-Glc steady-state labeling experiments (Salon et al. 1988). ^{14}C-labeling has also been used to understand the metabolism of sucrose and starch in banana (Hill and ap Rees 1995) and potato tubers (Geigenberger et al. 1997) in response to hypoxia and hydric stress, respectively. On the one hand, this method is convenient because it does not require high-tech apparatus and is quite sensitive. On the other hand, it is time-consuming, requires the purification of metabolic intermediates for ^{14}C-analysis, and the information obtained is often limited to the average ^{14}C-labeling of the molecule. Protocols have been proposed to cleave the molecules of interest to get information on fragments or specific carbon positions. For instance, the specific isotopic content in the C-1 atom position of glucose has been determined after enzymatic decarboxylation: glucose was incubated in a sealed vial with hexokinase, glucose 6-phosphate dehydrogenase and 6-phosphogluconate dehydrogenase and evolved CO_2 was fixed with KOH (Hill and ap Rees 1994; Dieuaide-Noubhani et al. 1995). To investigate the redistribution of ^{14}C from C-1 to C-6, purified hexoses were enzymatically degraded to 3-phosphoglycerate and glycerol-3-phosphate and then separated by HPLC (Hatzfeld and Stitt 1990).

Since the 80s, NMR and LC-MS techniques made the use of ^{13}C-labeled substrates preferable, and this has several advantages. First of all, it became possible to analyze complex mixtures avoiding fastidious steps of purification prior labeling analysis. Moreover, data quality and quantity have been seriously improved. ^{13}C-NMR spectra can be used to quantify the ^{13}C labeled pool size of a molecule of interest, but it has to be coupled to another approach (^{1}H-NMR, HPLC…) to estimate the total pool size. Alternatively, the specific labeling of each single protonated carbon atom position inside a metabolite can be easily determined from ^{1}H-NMR spectra, alone or coupled to ^{13}C-NMR spectra when protons are not resolved in the first one. Using two-dimen-

sional [^{13}C,^{1}H]-NMR, the isotopomer distribution is even more resolved, but precautions have to be taken to assure quantitative analysis. Using high resolution (accurate mass) LC-MS, isotopic patterns (M, M + 1, M + 2, etc.) can be analyzed and thereby isotopomer distribution can be determined. This gain in information is beneficial for the accuracy of network definition (^{13}C-redistribution) and flux quantitation (Massou et al. 2007).

Metabolic maps were reconstructed from ^{13}C-labeling in several organisms: maize root tips (Dieuaide-Noubhani et al. 1995; Alonso et al. 2005, 2007a), *Catharanthus roseus* hairy roots (Sriram et al. 2007), tomato (Rontein et al. 2002) and *Arabidopsis* (Williams et al. 2008) cells, and various seed embryos (Sriram et al. 2004; Schwender et al. 2006; Junker et al. 2007; Lonien and Schwender 2009; Alonso et al. 2007b 2010). In all of these papers, the overall strategy was similar, that is, continuous labeling up to isotopic steady-state with ^{13}C-Glc as a carbon source, and then metabolic flux network modeling. However, there are major differences in the list of targeted metabolites and the nature of the information obtained from labeling. For example, fluxes in primary metabolism were quantified from either ^{13}C-enrichments in carbon atom positions in free sugars, starch, glutamate and aspartate determined by ^{1}H and ^{13}C-NMR (Dieuaide-Noubhani et al. 1995; Alonso et al. 2005, 2007a; Rontein et al. 2002), or isotopomer distribution in proteinogenic amino acids (obtained from protein hydrolysis) by 2D [^{13}C,^{1}H]-NMR (Sriram et al. 2004, 2007). To increase information redundancy and improve constraints applied to flux calculation, the tendency is now to explore a wide range of metabolites such as sugars, free and/or proteinogenic amino acids and also lipids using complementary techniques: NMR, LC- and GC-MS (Schwender et al. 2006; Junker et al. 2007; Lonien and Schwender 2009).

B. Behavior of the Tracer Upon Labeling: Dynamic Versus Steady-State Labeling

Most MFA studies in plants are based on steady-state labeling experiments, where the biological system of interest (tissue or cells) is in a stationary metabolic state with constant intracellular fluxes during the whole timeframe of the experiment. In practice, the ^{13}C-labeling period should be long enough to ensure that the labeling (% ^{13}C) in metabolites does not vary anymore. This method has two advantages. First, the isotopic content in metabolites (and C atom positions) can be described by linear equations that can be solved easily. Second, in the isotopic steady-state, the labeling in metabolites involved in the same linear metabolic pathway is identical; the isotopic enrichment differs between metabolites of the same pathway if there is a metabolic branching point thereby introducing more ^{13}C or causing an isotopic dilution. Consequently, a minimal dataset is required to estimate fluxes (Dieuaide-Noubhani et al. 1995) and targeted, easily detectable molecules can be analyzed instead of their precursors to get sufficient information. For example, when ^{13}C-glucose is used as the supplied isotopic tracer, the isotopic enrichment in sucrose, starch and glutamate reflects that in cytosolic glucose-6-phosphate (and fructose-6-phosphate), plastidial glucose-6-phosphate and 2-oxoglutarate, respectively. However, the experimental design requires particular attention because plant organs or tissues are often isolated from the mother plant and have to be cultivated in mediums that reproduce as much as possible biological conditions found *in planta*. For instance, embryos are cultivated on nutrient solutions that allow growth rate (Alonso et al. 2007b, 2010; Lonien and Schwender 2009). Another difficulty is that the time needed to reach the isotopic steady-state is often very long, from one day in maize root tips to several days for embryos or isolated cells. This is due to the

slow exchange process between the cytosol and the vacuole, which contains large amount of slowly turned-over metabolites. With such long labeling times *ex planta*, the primary carbon metabolism might vary during the experiment, and this is not compatible with the requirement for a metabolic and isotopic steady-state.

In the past decade, a strategy based on the analysis of labeling kinetics in tissues or cells that are in the metabolic steady-state (INST-^{13}C-MFA) has been developed (Wiechert and Noh 2005). Experimentally, this approach requires the collection of samples at different time points. It exploits the relatively high sensitivity of LC-MS analyses that allows analyzing metabolites even at low concentration and ^{13}C-enrichment. The general principle used to estimate flux distribution and quantification is then based on a least-square fit of observed data to equations that describe isotopomers kinetics. An advantage of INST-^{13}C-MFA is the possibility to discriminate between parallel pathways that lead to the same product, as long as their intermediates are different and can be analyzed.

However, numerical resolution of flux values that provide the best match to observed data is highly demanding in computational power and may be mathematically complicated (to find best converging algorithms). Therefore, labeling kinetics experiments have been successfully applied to study relatively small networks, like the benzenoid network in *Petunia* flowers (Colón et al. 2010) or cell wall metabolism in maize embryos (Chen et al. 2013). It should be noted that autotrophic organisms are well suited for INST-MFA because their metabolism is based on CO_2 assimilation and thus, $^{13}CO_2$ steady-state experiments cannot be used because all of the metabolic intermediates are eventually completely labeled. Methods for $^{13}CO_2$ labeling experiments coupled with INST-MFA modeling were first described in Shastri and Morgan (2007) and more recently applied to a plant model, the *Arabidopsis* leaves (Szecowka et al. 2013). However, they restricted their study to the Calvin cycle and its major derivatives. To deal with the complexity of metabolic networks and the associated mathematical treatment, Antoniewicz et al. (2007) and Young et al. (2008) proposed a theory based on the decomposition of the isotopomer redistribution network into elementary metabolite units (EMU). The authors consider that this approach reduces by a factor 10 the number of ordinary differential equations to solve, saving time and computing power in flux estimation. It was successfully used to determine fluxes in the cyanobacterium *Synechocystis* (Young et al. 2011). Recently, Young (2014) proposed a publicly available software package, INCA, to calculate fluxes from metabolic steady-state and non-stationary labeling experiments (INCA; http://mfa.vueinnovations.com/).

III. The Origin of Acetyl-CoA for the TCA Cycle

In plant heterotrophic tissues, it is generally accepted that sugars are the major source of carbon feeding respiration, so that their complete oxidation through glycolysis and the TCA cycle provides reductants (NADH and $FADH_2$). However, the nature of the respiratory substrate may vary, as described below. The respiratory quotient (RQ) is the ratio of moles of CO_2 produced to moles of O_2 consumed. The RQ has been used for more than one century to trace the carbon source used by respiration. A RQ close to one indicates that carbohydrates (glucose) are the major source of CO_2, whereas it equals ≈0.8 for proteins degradation and 0.6 during lipid oxidation (and less than 0.5 if gluconeogenesis is involved). Alternatively, an increase of the RQ above 1 suggests that fermentation occurs. Nevertheless, if the determination of the RQ value is pertinent to highlight changes in the nature of the respiratory substrate (e.g. Bathellier et al. 2009 in roots), it is not suf-

ficient to define precisely the substrate for respiration that can be sustained by a mixture of compounds, for instance lipids and organic and amino acids, so that the observed RQ is an average value.

A. Fatty Acids Degradation Sustains Respiration in Oil-Containing Seeds During Germination

In lipid-rich seeds, lipids that are stored during seed development are degraded to acetyl-CoA *via* β-oxidation during germination. Acetyl-CoA is then converted to sugars through the glyoxylate cycle and neoglucogenesis (Canvin and Beevers 1961). Both gluconeogenesis-derived sugars and succinate produced by the glyoxylic cycle are eventually used for biosyntheses as well as respiration. The role of fatty acids in germination and seedling development has been extensively studied in *Arabidospis thaliana* using mutants (Hayashi et al. 1998; Eastmond et al. 2000; Germain et al. 2001; Cornah et al. 2004; Pracharoenwattana et al. 2005). Surprisingly, the glyoxylic cycle does not appear to be essential for germination itself, but for post-germinative growth. In fact, when isocitrate lyase (which catalyzes one step of the glyoxylic cycle) is absent, seedling growth is reduced (because gluconeogenesis is impaired) but not suppressed, thanks to the use of fatty acid degradation products by respiration (Eastmond et al. 2000; Germain et al. 2001). That is, acetyl-CoA is converted to citrate by the peroxisomal citrate synthase and then exported to the mitochondrion to sustain the TCA cycle (Pracharoenwattana et al. 2005).

However, in other species, fatty acids are used in early germination events. Raymond et al. (1992) showed that a particulate fraction isolated from sunflower (*Helianthus annuus*) seeds is able to convert fatty acids to citrate when oxaloacetate is supplied. Salon et al. (1988) modeled the carbon provision to the TCA cycle in lettuce seeds and showed the importance of gluconeogenesis. This work is important since it represents the very first work dealing with plant fluxomics. It was based on steady-state ^{14}C-labeling experiments. As expected, they observed a production of ^{14}C-labeled carbohydrates after incubation of embryos with ^{14}C-acetate and ^{14}C-fatty acids. This simply reflected a flux towards gluconeogenesis. But surprisingly, the rate of ^{14}C-labeled CO_2 evolution was much larger than the flux associated with gluconeogenesis. Three pathways could have explained this effect: *(i)* α-oxidation, that produces directly CO_2 from the α carbon of fatty acids, *(ii)* the 'classical' pathway coupling β-oxidation to the glyoxylate cycle or *(iii)* direct utilization of acetyl-CoA (produced by β-oxidation) by citrate synthase to sustain the TCA cycle. The authors elegantly discriminated these three pathways by looking at the ^{14}C ratio aspartate-to-glutamate after incubation with ^{14}C-labeled acetate, palmitate and hexanoate. From a theoretical point of view, if fatty acids were degraded by β-oxidation and further metabolized in the glyoxylic cycle only, the labeling would enter the TCA cycle through C_4 intermediates only. In this case, the four carbons of aspartate would be labeled. In glutamate, only three carbon atoms coming from OAA would be labeled and not those originating from acetyl-CoA *via* citrate synthase (see Fig. 12.2). Therefore, the isotope ratio aspartate-to-glutamate would have to be $4/3 = 1.33$. By contrast, if acetyl-CoA were essentially metabolized by citrate synthase, then all of the carbon atom positions in glutamate and aspartate would be labeled and the ratio would equal $4/5 = 0.8$. For all of the substrates tested, the ratio measured was close to 0.8, indicating that fatty acids were degraded by β-oxidation and incorporated as acetyl-CoA (rather than C_4 intermediates) into citrate to sustain respiration. This was further confirmed by short-time labeling that showed that when embryos were incubated with ^{14}C-hexanoate, citrate and glutamate were much more rapidly labeled than malate and aspartate.

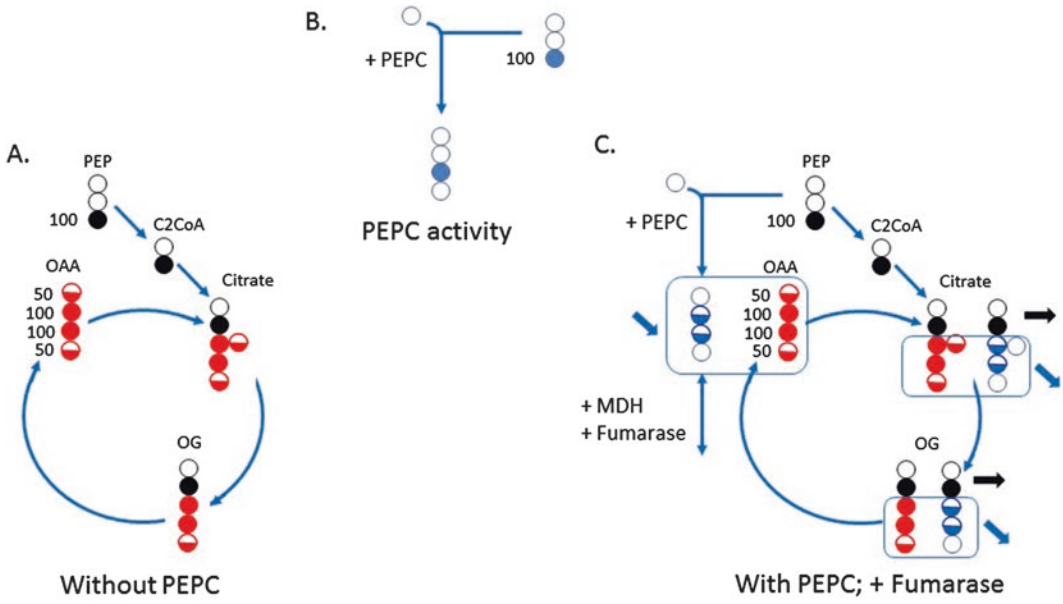

Fig. 12.2. **Impact of PEPC activity on the specific labeling of TCA cycle intermediates at the isotopic steady-state.** In **a**, citrate is formed from acetyl-CoA (C2CoA) originating from PEP. Arbitrary, the labeling of the C-3 of PEP is 100, whereas the two other carbons are not labeled. The PEPC activity combines PEP with CO_2 thus producing OAA labeled on C-3 only (**b**). Due to the malate dehydrogenase and fumarase activities, the OAA produced from the PEPC is labeled on carbons C-2 and C-3 (**c**). The specific labeling of all OAA carbons is reduced (blue arrow). Consequently, the specific labeling of the carbons of the lower part of citrate and oxoglutarate is also reduced whereas the carbons from the upper part, coming from acetyl-CoA are not affected (black arrow)

B. Fatty Acids and Proteins Are Respiratory Substrates Under Sugar Limitation

In maize root tips (Saglio and Pradet 1980; Brouquisse et al. 1991), sycamore (*Acer pseudoplatanus*) cells (Journet et al. 1986) or tomato roots (Devaux et al. 2003), sugar removal (glucose or sucrose) from the culture medium leads to a decrease in the respiration rate and fatty acid and protein content, suggesting that they play the role of alternative respiratory substrates (Saglio and Pardet 1980). They represent the sole carbon source after 15 h of sugar starvation, since the pool in soluble sugars does not vary anymore (Brouquisse et al. 1991). These conclusions based on metabolite contents have been corroborated by the increase in protease (James et al. 1993) and β-oxidation (Dieuaide et al. 1992) activities (but not in glyoxylic cycle activity), and the decrease in RQ from ≈1 to 0.7 in a few hours (Dieuaide-Noubhani et al. 1997).

To understand the metabolic reorchestration during starvation and identify the role played by fatty acids and proteins in sustaining the TCA cycle, detached maize root tips were labeled for 4 h with [^{13}C-1]-Glc, just the time required to label glycolysis and TCA cycle intermediates but not lipids and proteins. Alanine (C-3 atom position) and glutamate (C-4 atom position) were found to be identically ^{13}C-labeled, reflecting the fact that sugars were the sole carbon source for the TCA cycle. When roots were transferred to a glucose-free medium, a continuous decrease in the ^{13}C-labeling of glutamate C-4 was observed while alanine C-3 remained almost stable. Unfortunately, under sugar

starvation conditions, quantitative MFA was not applicable because both cells were not at the metabolic and isotopic steady-state. However, a qualitative interpretation remains possible: the decrease in glutamate C-4 as compared to alanine C-3 suggests the utilization of an unlabeled (^{12}C) carbon source by the TCA cycle, probably fatty acids or proteins recycling. The authors also observed that the ^{13}C-labeling of the three carbon atom positions C-2, C-3, and C-4 in glutamate was identical after 6 h of starvation. This indicates that the incorporation of the unlabeled carbon source was unlikely to be between citrate and glutamate (i.e., with a branching point within the TCA cycle) since it would have had a ^{13}C-diluting effect in the C-2 and C-3 atom positions as well. In other words, fatty acids were used as carbon substrates to generate acetyl-CoA and thus sustain the TCA cycle, and 2-oxoacids from protein degradation were used marginally.

Interestingly, a similar metabolic response has been observed in leaves subjected to continuous darkness, with an increase in transcripts encoding for β-oxidation enzymes, but not for the glyoxylate cycle like malate synthase and isocitrate lyase (Tcherkez et al. 2003; Pracharoenwattana et al. 2005; van der Graaff et al. 2006; Kunz et al. 2009).

IV. The TCA Cycle: Anaplerotic Pathways *Versus* Catabolism

A. PEP Carboxylation, the Major Anaplerotic Pathway

In principle, if [^{13}C-1]-Glc (or sucrose) were the sole carbon source, in the absence of anaplerotic pathway, the carbon atom positions C-2, C-3 in OAA and C-2, C-3, C-4 in 2-oxoglutarate (and thus in glutamate) would be identically labeled to C-3 of PEP derived from glycolysis. The C-1 atom position in glutamate should not be labeled since it originates from C-2 in PEP (and thus C-1 in acetyl-CoA), which is not labeled upon [^{13}C-1]-Glc labeling. By contrast, PEPC activity produces OAA which harbors labeling on the C-3 atom position, which in turn directly comes from the C-3 of PEP. This position in OAA is then rapidly randomized between the carbon atom positions C-2 and C-3 by fumarase, because fumarate is symmetrical and the reaction between malate and fumarate is reversible. Consequently, this leads to an isotopic dilution whereby the isotopic content in C-2 and C-3 represents one half of that in the C-3 atom position of PEP. In other words, PEPC-derived OAA should isotopically dilute TCA-derived OAA and thus also in corresponding C-atom positions in 2-oxoglutarate and glutamate. This does not affect the C-4 and C-5 atom positions in glutamate since they originate from acetyl-CoA (Fig. 12.2). Therefore, the ^{13}C-dilution in C-2 and C-3 with respect to C-4 reflects the PEPC activity and allows estimating the ratio PEPC/PDH (pyruvate dehydrogenase), once the external fluxes from TCA cycle have been estimated. This last point is usually achieved by measuring the rate of protein synthesis and the relative abundance of each amino acid in proteins.

The carbon allocation from the TCA cycle to energy generation (respiratory CO_2 release) and to biosynthesis (e.g. amino acids production) has been determined in several plant species. In standard conditions, the ratio PEPC/PDH was found to vary slightly between 0.37 in *Arabidopsis* cells and soybean embryos, and 0.6 in maize root tips or embryos (Table 12.1). This indicates that the fate of TCA cycle intermediates may vary considerably between species. In addition, the ratio PEPC/PDH can be affected by environmental conditions. In maize root tips (Dieuaide-Noubhani et al. 1997) and tomato cells (Rontein et al. 2002), the response to decreased carbon availability has been examined either directly by incubating maize roots in the absence of glucose or indirectly by observing the consequence of progressive glucose consumption when tomato cells were

Table 12.1. PEPC/PDH ratios in plant tissues

	Maize root tips[a]	Tomato cells[b]	*Arabidopsis* Cells[c]	Sunflower embryos[d]	*Brassica napus* embryos[e]	Soybean embryos[f]	*C. Roseus* hairy roots[g]
				PEPC/PDH			
Standard growth	0.5/0.6	0.48	0.37	0.6	0.6	0.38	0.23
Carbon limiting	0	0.31 to 0.25					
Elevated O_2			0.29				

Values are calculated from (a) Dieuaide-Noubhani et al. (1995), (b) Rontein et al. (2002), (c) Williams et al. (2008), (d) Alonso et al. (2007b), (e) Junker et al. (2007), (f) Sriram et al. (2004), and (g) Sriram et al. (2007)

batch-cultivated. In both cases, a rapid decrease in the respiration rate has been observed. In maize root tips, glucose depletion led to a clear arrest of PEPC activity as well as growth. In tomato cells in the pre-stationary phase, the flux through the PEPC decreased by 80% while the flux through the PDH decreased by 60%, thus favoring catabolism over anaplerosis. In *Arabidospsis* cells incubated under elevated O_2, cell growth was improved and all fluxes increased. However, relative fluxes were only slightly modified, the ratio between catabolism and biosynthesis being almost not affected (Williams et al. 2008). This is consistent with the assumption that flux patterns in primary carbon metabolism are relatively stable, that is, respond to environmental perturbations with limited flux redistribution.

B. Amino Acids as a Carbon Source

Many heterotrophic tissues derive their nitrogen from amino acids. This is typically the case in seed embryos that transport amino acids provided by parental tissues. In this form, nitrogen is reduced and can be directly used in metabolism *via* transamination. Considering the nitrogen source (mineral *versus* organic) is crucial not only because meeting nutritional requirements influences growth but also because amino acids are also a carbon source that may enter primary metabolism and sustain the TCA cycle, thus playing the role of an anaplerotic pathway. Junker et al. (2007) compared growth and metabolic fluxes in *Brassica napus* embryos cultivated with alanine + glutamine or ammonium + nitrate as an organic and inorganic nitrogen source, respectively. When inorganic N was used, they observed a significant decrease in growth and protein accumulation (reduced by 25%) but an increase in lipids (+12%). This effect was possibly due to the utilization of reducing power to assimilate nitrogen at the expense of biosyntheses. Conversely, with an organic N source, embryos required less sugar-derived carbon to synthesize amino acids and proteins. Moreover, since almost 30% of glutamine entered the TCA cycle as 2-oxoglutarate, thus playing the role of an anaplerotic function, the flux through the PEPC was decreased considerably. Therefore, in *Brassica napus* embryos, the TCA cycle appears to be influenced by the N source. With inorganic N, the TCA cycle operates as a circle as classically described in textbooks while with organic N, the flux through the isocitrate dehydrogenase is severely decreased and even reversed. In fact, isocitrate dehydrogenation can be catalyzed by two enzyme activities, one being NAD-dependent and irreversible (IDH) and one NADP-dependent and readily reversible (ICDH). In the present case, ICDH is presumably favored upon organic N feeding.

As a consequence, under organic N conditions, ATP produced by oxidative phosphorylation in mitochondria accounts for 22% only of ATP required for biosyntheses (Schwender et al. 2006). However, it should be noted that this flux pattern is not a general behaviour. For instance, in *Arabidopsis*

embryos (Lonien and Schwender 2009), sunflower embryos (Alonso et al. 2007b) or maize embryos (Alonso et al. 2010), all cultivated with sugars and amino acids, the flux through isocitrate dehydrogenase favors the 'classical' TCA cycle. This contrasting result could be partly explained by the relatively high ATP requirements in *Arabidopsis* embryos due to higher protein content. This would be especially true in the mutant used in that study (*wrinkle1*), since it accumulates twice as much protein and shows a fourfold increase in isocitrate dehydrogenase activity (Lonien and Schwender 2009). On the other hand, the case of maize embryos is specific because they accumulate more starch (about 30% of the dry weight) and less protein (only 6%). That is, the carbon source is mostly used to synthesize starch and absorbed in the form of sugars: only 7% of carbon is absorbed as amino acids, while this proportion is 15 and 20% in *Brassica napus* and *Arabidopsis* embryos, respectively.

C. The Malic Enzyme Redirects Anaplerotic Carbon to Respiration

The malic enzyme (ME) is present in three sub-cellular compartments in plants (plastids, mitochondria and cytosol). It catalyzes the conversion of malate to pyruvate + CO_2 and generates NADH (cytosolic and mitochondrial isoforms) or NADPH (plastids). It is believed that the plastidial isoform (pME) plays an important role in reductant supply for fatty acids synthesis whereas the mitochondrial isoform (mME) is associated with catabolism. ME activity is often low in tissues that do not accumulate oil (Dieuaide-Noubhani et al. 1995; Alonso et al. 2007a). However, in *C. roseus* hairy roots, the flux through mME has been found to be relatively high and most of the carbon entering the TCA cycle *via* the PEPC is converted to pyruvate *via* mME activity (Sriram et al. 2007). Considering that OAA evolved by the PEPC is converted to malate in the cytosol before being imported into the mitochondria, the authors suggested that this metabolic pathway could be part of a mechanism to import reductive power. That way, the cytosolic malate dehydrogenase (cMDH) would generate NAD^+ from NADH (thereby reducing OAA in malate) whereas mitochondrial malate dehydrogenase (mMDH) and mME would generate NADH from malate oxidation to OAA and pyruvate, respectively. In maize embryos that accumulate 34% of carbon as lipids, it has been shown that the flux trough the pentose phosphate pathway cannot generate enough NADPH to sustain fatty acids synthesis at a high rate and one third of required NADPH is provided by pME (Alonso et al. 2010). By comparing pME activity measured *in vitro* (163 nmol h^{-1} $embryo^{-1}$) and the effective flux (175 nmol h^{-1} $embryo^{-1}$), the authors further suggested that the enzyme could be rate-limiting for fatty acids biosynthesis and thus a target for engineering oil composition in maize grains.

In seed embryos of the *Arabidopsis* mutant *wrinkled1*, the flux through plastidial pyruvate kinase has been shown to be reduced fivefold and seed oil content threefold (Lonien and Schwender 2009). However, ME activities were increased, suggesting that pyruvate biosynthesis was achieved by PEPC followed by mME and pME instead of glycolysis, thereby providing NADPH for fatty acids synthesis. mME would then sustain NADH production and thus mitochondrial ATP production for biosyntheses.

V. Concluding Remarks

Understanding how the TCA cycle operates is essential because beyond the classical view as just a circle, it is the cornerstone of both ATP generation and biosyntheses and thus, it is at the heart of metabolic interactions with anaplerosis and other pathways. Our ability to understand its role and identify regulatory points depends on our ability to quantify fluxes. ^{13}C-MFA provides a conve-

nient way to determine fluxes, including that associated with carbon entry into the TCA cycle. Having said that, although the methodology is now well documented (including practical guidelines for performing and publishing ^{13}C-MFA, Crown and Antoniewicz 2013), its application to plant tissues remains rather limited. The main reason has to do with the practical difficulty to reach the isotopic steady-state due to slow turn-over metabolic pools. The recent development of INST-MFA is likely to provide solutions to perform fluxomics analyses in plants. Also, methods that use carbon isotopes at natural abundance (^{12}C/^{13}C ratios) are likely to provide insightful data on respiratory metabolism in heterotrophic plant cells. These approaches using natural abundance isotope and intramolecular isotopic composition analysis are presented in Chap. 3.

References

Alonso AP, Vigeolas H, Raymond P, Rolin D, Dieuaide-Noubhani M (2005) A New Substrate Cycle in Plants: Evidence for a High Glucose-Phosphate - Glucose Turnover from *in Vivo* Steady State and Pulse Labeling Experiments with [^{13}C]- and [^{14}C] Glucose. Plant Physiol 138:2220–2232

Alonso AP, Goffman FD, Ohlrogge JB, Shachar-Hill Y (2007a) Carbon conversion efficiency and central metabolic fluxes in developing sunflower (*Helianthus annuus* L.) embryos. Plant J 52:296–308

Alonso AP, Raymond P, Hernould M, Rondeau-Mouro C, de Graaf A, Chourey P, Dieuaide-Noubhani M (2007b) A metabolic flux analysis to study the role of sucrose synthase in the regulation of the carbon partitioning in central metabolism in maize root tips. Metab Eng 9:419–432

Alonso AP, Dale VL, Shachar-Hill Y (2010) Understanding fatty acid synthesis in developing maize embryos using metabolic flux analysis. Metab Eng 12:488–497

Antoniewicz MR, Kelleher JK, Stephanopoulos G (2007) Elementray metabolite units (EMU): a novel framework for modeling isotopic distributions. Metab Eng 9:68–86

Baghalian K, Hajirezaei MR, Schreiber F (2014) Plant metabolic modeling: achieving new insight into metabolism and metabolic engineering. Plant Cell 26:3847–3866

Bathellier C, Tcherkez G, Bligny R, Gout E, Cornic G, Ghashghaie J (2009) Metabolic origin of the δ^{13}C of respired CO_2 in roots of *Phaseolus vulgari*. New Phytol 181:387–399

Beauvoit BP, Colombié S, Monier A, Andrieu MH, Biais B, Bénard C, …, Gibon Y (2014) Model-Assisted Analysis of Sugar Metabolism throughout Tomato Fruit Development Reveals Enzyme and Carrier Properties in Relation to Vacuole expansion. Plant Cell 26: 3224--3242.

Brouquisse R, James F, Raymond P et al (1991) Study of glucose starvation in excised maize root tips. Plant Physiol 96:619–626

Canvin DT, Beevers H (1961) Sucrose synthesis from acetate in the germinating castor bean: kinetics and pathway. J Biol Chem 236:988–995

Chen X, Alonso AP, Shachar-Hill Y (2013) Dynamic metabolic flux analysis of plant cell wall synthesis. Metab Eng 18:78–85

Colombié S, Nazaret C, Bénard C, Biais B, Mengin V, Solé M, …, Gibon Y. (2015) Modeling central metabolic fluxes by constraint-based optimization reveals metabolic reprogramming of developing *Solanum lycopersicum* (tomato) fruit. Plant J. 81: 24--39.

Colón AM, Sengupta N, Rhodes D, Dudareva N, Morgan J (2010) A kinetic model describes metabolic response to perturbations and distribution of flux control in the benzenoid network of Petunia hybrid. Plant J 62:64–76

Cornah JE, Germain V, Ward JL, Beale MH, Smith SM (2004) Lipid utilization, gluconeogenesis, and seedling growth in *arabidopsis* mutants lacking the glyoxylate cycle enzyme malate synthase. J Biol Chem 279:42916–42923

Crown SB, Antoniewicz MR (2013) Publishing ^{13}C metabolic flux analysis studies: A review and future perspectives. Metab Eng 20:42–48

Curien G, Ravanel S, Dumas R (2003) A kinetic model of the branch-point between the methionine and threonine biosynthesis pathways in Arabidopsis thaliana. Eur J Biochem 270:4615–4627

Curien G, Bastien O, Robert-Genthon M, Cornish-Bowden A, Cárdenas ML, Dumas R (2009) Understanding the regulation of aspartate metabolism using a model based on measured kinetic parameters. Mol Sys Biol 5:271–281

de Oliveira Dal'Molin CG, Quek LE, Palfreyman RW, Brumbley SM, Nielsen LK (2010) AraGEM, a genome-scale reconstruction of the primary metabolic network in Arabidopsis. Plant Physiol 152:579–589

de Oliveira Dal'Molin CG, Quek LE, Saa PA, Nielsen LK (2015) A multi-tissue genome-scale metabolic modeling framework for the analysis of whole plant systems. Front Plant Sci 6:4

Dersch LM, Beckers V, Wittmann C (2016) Green pathways: Metabolic network analysis of plant systems. Metab Eng 34:1–24

Devaux C, Baldet P, Joubès J, Dieuaide-Noubhani M, Just D, Chevalier C, Raymond P (2003) Physiological, biochemical and molecular analysis of sugar-starvation responses in tomato roots. J Exp Bot 54:1143–1151

Dieuaide M, Bouquisse R, Pradet A, Raymond P (1992) Increased fatty acid beta-oxidation after glucose starvation in maize root tips. Plant Physiol 99:595–600

Dieuaide-Noubhani M, Alonso AP (2014) Plant metabolic flux analysis: methods and protocols. In: Dieuaide-Noubhani M, Alonso AP (eds) Methods in molecular biology, vol 1090. Humana Press-Springer, Berlin, pp 1–17

Dieuaide-Noubhani M, Raffard G, Canioni P, Pradet A, Raymond P (1995) Quantification of compartmented metabolic fluxes in maize root tips using isotope distribution from ^{13}C- or ^{14}C-labeled glucose. J Biol Chem 270:13147–13159

Dieuaide-Noubhani M, Canioni P, Raymond P et al (1997) Sugar-starvation-induced changes of carbon metabolism in excised maize root tips. Plant Physiol 115:1505–1513

Droste P, Miebach S, Niedenfuhr S, Wiechert W, Noh K (2011) Visualizing multi-omics data in metabolic networks with the software Omix-A case study. Biosystems 105:154–161

Eastmond PJ, Germain V, Lange PR, Bryce JH, Smith SM, Graham IA (2000) Postgerminative growth and lipid catabolism in oilseeds lacking the glyoxylate cycle. Proc Natl Acad Sci USA 97:5669–5674

Geigenberger P, Reimholz R, Geiger M, Merlo L, Canale V, Stitt M (1997) Regulation of sucrose and starch metabolism in potato tubers in response to short-term water deficit. Planta 201:502–518

Germain V, Rylott EL, Larson TR, Sherson SM, Bechtold N, Carde JP et al (2001) Requirement for 3--ketoacyl-CoA thiolase-2 in peroxisome development, fatty acid β-oxidation and breakdown of triacylglycerol in lipid bodies of Arabidopsis seedlings. Plant J 28:1–12

Grafahrend-Belau E, Schreiber F, Koschützki D, Junker BH (2009) Flux balance analysis of barley seeds: a computational approach to study systemic properties of central metabolism. Plant Physiol 149:585–598

Grafahrend-Belau E, Junker A, Eschenroder A, Muller J, Schreiber F, Junker BH (2013) Multiscale metabolic modeling: dynamic flux balance analysis on a whole-plant scale. Plant Physiol 163:637–647

Hatzfeld WD, Stitt M (1990) A study of the rate of recycling of triose phosphates in heterotrophic *Chenopodium rubrum* cells, potato tubers, and maize endosperm. Planta 180:198–204

Hayashi M, Toriyama K, Kondo M, Nishimura M (1998) 2,4--dichlorophenoxybutyric acid-resistant mutants of arabidopsis have defects in glyoxysomal fatty acid beta-oxidation. Plant Cell 10:183–195

Hill SA, ap Rees T (1994) Fluxes of carbohydrate metabolism in ripening bananas. Planta 192:52–60

Hill SA, ap Rees T (1995) The effect of hypoxia on the control of carbohydrate metabolism in ripening bananas. Planta 197:313–323

James F, Brouquisse R, Pradet A, Raymond P (1993) Changes in proteolytic activities in glucose-starved maize root tips – regulation by sugars. Plant Physiol Biochem 31:845–856

Journet EP, Bligny R, Douce R (1986) Biochemical changes during sucrose deprivation in higher plant cells. J Biol Chem 261:3193–3199

Junker BH, Lonien J, Heady LE, Rogers A, Schwender J (2007) Parallel determination of enzyme activities and *in vivo* fluxes in *Brassica napus* embryos grown on organic or inorganic nitrogen source. Phytochemistry 68:2232–2242

Kim TY, Sohn SB, Kim YB, Kim WJ, Lee SY (2012) Recent advances in reconstruction and applications of genome-scale metabolic models. Curr Op. Biotech 23:617–623

Kunz H-H, Scharnewski M, Feussner K, Feussner I, Flügge U-I, Fulda M, Giertha M (2009) The ABC transporter PXA1 and peroxisomal β-oxidation are vital for metabolism in mature leaves of Arabidopsis during extended darkness. Plant Cell 21:2733–2749

Lonien J, schwender J (2009) Analysis of metabolic flux phenotypes for two Arabidopsis mutants with severe impairment in seed storage lipid synthesis. Plant Physiol 151:1617–1634

Massou S, Nicolas C, Letisse F, Portais JC (2007) NMR-based fluxomics: Quantitative 2D NMR methods for isotopomers analysis. Phytochemistry 68:2330–2340

Pracharoenwattana I, Cornah JE, Smith SM (2005) Arabidopsis peroxisomal citrate synthase is required for fatty acid respiration and seed germination. Plant Cell 17:2037–2048

Raymond P, Spiteri A, Dieuaide M, Gerhardt B, Pradet A (1992) Peroxisomal β-oxidation of fatty acids and citrate formation by a particulate fraction from early germinating sunflower seeds. Plant Physiol Biochem 30:153–161

Rohwer JM, Botha FC (2001) Analysis of sucrose accumulation in the sugar cane culm on the basis of *in vitro* kinetic data. Biochem J 358:437–445

Rontein D, Dieuaide-Noubhani M, Dufourc EJ, Raymond P, Rolin D (2002) The metabolic architecture of plant cells. Stability of central carbon metabolism and flexibility of anabolic pathways during the growth cycle of tomato cells. J Biol Chem 46(43):948–43960

Saglio PH, Pradet A (1980) Soluble sugars, respiration and energy charge during aging of excised maize root tips. Plant Physiol 66:516–519

Saha R, Suthers PF, Maranas CD (2011) *Zea mays* iRS1563: a comprehensive genome-scale metabolic reconstruction of maize metabolism. PLOS ONE 6:e21784

Salon C, Raymond P, Pradet A (1988) Quantification of carbon fluxes through the tricarboxylic acid cycle in early germinating lettuce embryos. J Biol Chem 263:12278–12287

Schuster S, Dandekar T, Fell DA (1999) Detection of elementary flux modes in biochemical networks: a promising tool for pathway analysis and metabolic engineering. Trends Biotechnol 17:53–60

Schwender J, Shachar-Hill Y, Ohlrogge JB (2006) Mitochondrial metabolism in developing embryos of *Brassica napus*. J Biol Chem 281:34040–34047

Shastri AA, Morgan JA (2007) A transient isotopic labeling methodology for ^{13}C metabolic flux analysis of photoautotrophic microorganisms. Phytochemistry 68:2302–2312

Sriram G, Fulton DB, Iyer VV, Peterson JM, Zhou R, Westgate ME, Spalding MH, Shanks JV (2004) Quantification of compartmented metabolic fluxes in developing soybean embryos by employing biosynthetically directed fractional ^{13}C labeling, two-dimensional [^{13}C, ^{1}H] nuclear magnetic resonance, and comprehensive isotopomer balancing. Plant Physiol 136:3043–3057

Sriram G, Fulton DB, Shanks JV (2007) Flux quantification in central carbon metabolism of Catharanthus roseus hairy roots by ^{13}C labeling and comprehensive bondomer balancing. Phytochemistry 68:2243–2257

Szecowka M, Heise R, Tohge T, Nunes-Nesi A, Vosloh D, Huege J, …, Arrivault S (2013) Metabolic fluxes in an illuminated Arabidopsis rosette. Plant Cell 25: 694--714.

Tcherkez G, Nogués S, Bleton J, Cornic G, Badeck F, Ghashghaie J (2003) Metabolic origin of carbon isotope composition of leaf dark-respired CO_2 in French bean. Plant Physiol 131:237–244

van der Graaff E, Schwacke R, Schneider A, Desimone M, Flügge U-I, Kunze R (2006) Transcription analysis of Arabidopsis membrane transporters and hormone pathways during developmental and induced leaf senescence. Plant Physiol 141:776–792

Wiechert W, Noh K (2005) From stationary to instationary metabolic flux analysis. Adv Biochem Eng Biotechnol 92:145–172

Williams TCR, Miguet L, Masakapalli SK, Kruger NJ, Sweetlove JJ, Ratcliffe RG (2008) Metabolic network fluxes in heterotrophic Arabidopsis cells: stability of the flux distribution under different oxygenation conditions. Plant Physiol 148:704–718

Young JD (2014) INCA: a computational platform for isotopically non-stationary metabolic flux analysis. Bioinformatics 30:1333–1335

Young JD, Walther JL, Antoniewicz MR, Yoo H, Stephanopoulos G (2008) An elementary metabolite unit (EMU) based method of isotopically nonstationary flux analysis. Biotechnol Bioeng 99:686–699

Young JD, Shastri AA, Stephanopoulos G, Morgan JA (2011) Mapping photoautotrophic metabolism with isotopically nonstationary ^{13}C flux analysis. Metab Eng 13:656–665